Australian Meteorological and Oceanographic Journal 61 (2011) 185–195

Seasonal climate summary southern hemisphere (spring 2010): La Niña strengthens

Ceri Lovitt
National Climate Centre, Bureau of Meteorology, Australia

(Manuscript received July 2011)

Southern hemisphere circulation patterns and associated anomalies for the austral spring 2010 are reviewed, with emphasis given to the Pacific Basin climate indicators and Australian rainfall and temperature patterns. Spring 2010 saw a continued strengthening of the La Niña conditions which started to become apparent in the autumn. All ENSO indices were showing a strong La Niña signal throughout the spring, with the October value of the Southern Oscillation Index (SOI) equalling its highest value on record. The Southern Annular Mode (SAM) also remained strongly positive during spring 2010, with the SAM index setting a monthly record in November. Additionally, the observation based SAM index set a seasonal record in spring 2010. In the Australian region, spring 2010 was the wettest spring on record with above average rainfall across most of the country. In sharp contrast however, southwestern Australia reported its driest spring on record following on from the driest winter on record. Temperatures were generally cooler than average across central and southern Australia, with the widespread rainfall contributing to the cooler temperatures. Warmer temperatures were experienced in some northern and coastal regions.

Introduction

This summary reviews the southern hemisphere climate patterns for the austral 2010 spring (September to November). Australasian and Pacific regions are given particular attention in this discussion. The main sources of information for this summary were analyses prepared by the Australian Bureau of Meteorology's National Climate Centre and the Centre for Australian Weather and Climate Research (CAWCR).

ENSO and Pacific Basin climate indices

The Troup Southern Oscillation Index (SOI)[1]

The Troup Southern Oscillation Index (SOI) for the period January 2006 to December 2010 is shown in Fig. 1, together with a five-month weighted moving average. The SOI is calculated using the mean sea-level pressure (MSLP) from both Darwin and Tahiti. Persistent departures of the SOI from zero can reflect El Niño-Southern Oscillation (ENSO) events.

Autumn 2010 (March to May) saw the SOI rise rapidly, transitioning into a La Niña event (Campbell, 2011). During the austral winter, SOI values remained positive, leading into spring (Ganter, 2011). Spring values of the SOI became indicative of a strong and sustained La Niña event, with +25.0 for September (second highest September on record), +18.3 for October (equal highest October on record) and +16.4 in November. Spring monthly MSLP values at Darwin were below average, whilst values at Tahiti were above average. The monthly MSLP anomalies (based on the average over the period 1933–1992) for September, October and November in Darwin were –1.2, –1.4 and –0.3 hPa respectively. Corresponding values for Tahiti were +2.9 (September), +1.6 (October) and +2.2 hPa (November). Values from both sites contributed to the high SOI values during spring, however the high values at Tahiti had the greater effect.

Composite monthly ENSO index

A composite monthly ENSO index, calculated as the

[1]The Troup Southern Oscillation Index (Troup 1965) used in this article is ten times the standardised monthly anomaly of the difference in mean sea level pressure (MSLP) between Tahiti and Darwin. The calculation is based on a sixty-year climatology (1933–1992). The Darwin MSLP is provided by the Bureau of Meteorology, with the Tahiti MSLP being provided by Météo France inter-regional direction for French Polynesia.

Corresponding author address: Ceri Lovitt, National Climate Centre, Bureau of Meteorology, GPO Box 1289, Melbourne VIC 3001, Australia
email: C.Lovitt@bom.gov.au

standardised amplitude of the first principal component[2] of monthly Darwin and Tahiti MSLP[3] and monthly NINO3, NINO3.4 and NINO4 sea-surface temperatures[4] (SSTs) (Kuleshov et al. 2008), remained in negative values after a steady fall which began in April 2010 (Fig. 2). Sustained positive (negative) values are indicative of an El Niño (La Niña) event. All of the three spring values well exceeded one standard deviation, confirming that the continuing positive phase of the Southern Oscillation had reached La Niña status. Monthly values of this index were –2.00 (September), –1.82 (October) and –1.50 (November). The September value of this index was the most negative monthly value since February 2008 (–2.10), during the 2007–08 La Niña.

Fig. 1 Monthly Southern Oscillation Index, from January 2006 to December 2010, together with a five-month binomially weighted moving average. Means and standard deviations used in the computation of the SOI are based on the period 1933–1992.

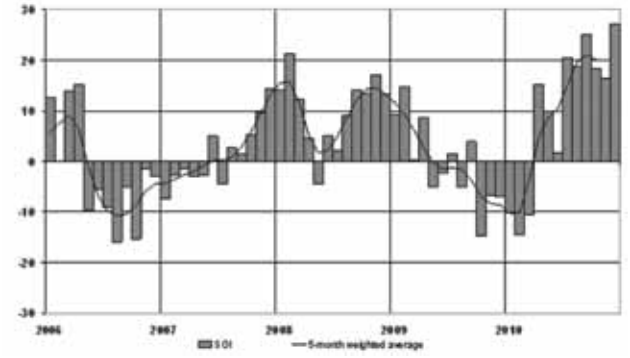

Fig. 2 Composite standardised monthly ENSO index from January 2006 to December 2010, together with a weighted three-month moving average. See text for details.

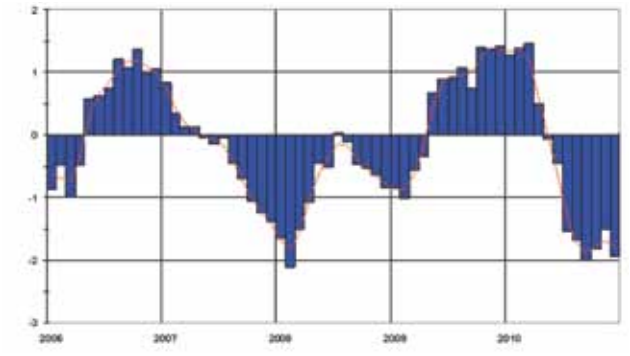

[2]The principal component analysis and standardisation of this ENSO index is performed over the period 1950-1999.
[3]MSLP data obtained from http://www.bom.gov.au/climate/current/soihtm1.shtml. As previously mentioned, the Tahiti MSLP data are provided by Météo France inter-regional direction for French Polynesia.
[4]SST indices obtained from ftp://ftp.cpc.ncep.noaa.gov/wd52dg/data/indices/sstoi.indices

Multivariate ENSO index

The Multivariate ENSO Index[5] (MEI), produced by the US Climate Diagnostics Center, is derived from a number of atmospheric and oceanic parameters typically associated with ENSO and is calculated as a two-month mean (Wolter and Timlin 1993, 1998). Significant negative values indicate La Niña, while significant positive values indicate El Niño. The MEI values have been ranked over the 61 year record, beginning in 1950. The lowest value (1) signifies the strongest La Niña case for that particular two month pairing, while the highest number (61) signifies the strongest El Niño case. The MEI remained consistently negative from the May–June 2010 value of –0.434, the first negative value after a sequence of thirteen positive values. A strong negative value of –2.017 in August–September was ranked 1, indicating that the 2010 La Niña could be one of the strongest in the MEI history (Climate Diagnostics Center 2010). The September–October value of –1.937 was ranked 2, whilst the October–November value of –1.577 was ranked 3. The August–September 2010 value was the most negative value recorded in any month since July–August 1955.

Outgoing long-wave radiation

Outgoing long-wave radiation (OLR) over the equatorial Pacific near the Date Line (5ºS to 5ºN and 160ºE to 160ºW) is a good measure of tropical deep convection, with increases (decreases) in OLR indicating decreases (increases) in convection. During La Niña events, OLR is often increased, meaning convection is often suppressed over this region. El Niño events on the other hand, usually have decreased OLR, meaning convection is generally enhanced over this region. The Climate Prediction Center, Washington, computes a standardised monthly anomaly[6] of OLR over the equatorial Pacific. Monthly values for September, October and November were +1.5, +1.5 and +1.7, respectively. The seasonal mean for spring was +1.6, the highest spring value on record (records began in 1974). The strongly positive values are consistent with La Niña conditions, and indicate that there was decreased convection over the equatorial Pacific.

The spatial pattern of seasonal OLR anomalies across the Asia-Pacific tropics for spring 2010 is shown in Fig. 3. Consistent with the standardised anomalies discussed above, very strong positive anomalies were present in the western equatorial Pacific. Very strong negative OLR anomalies were present over Indonesia, indicating that there was increased convection over the region during September to November. This pattern was well aligned with that expected during La Niña events. Negative OLR anomalies

[5]Multivariate ENSO Index obtained from http://www.esrl.noaa.gov/psd/people/klaus.wolter/MEI/table.html. The MEI is a standardised anomaly index.
[6]Standardised monthly OLR anomaly data obtained from http://www.cpc.ncep.noaa.gov/data/indices/olr

Fig. 3 OLR anomalies for spring 2010 in W m^{-2}. Base period is from 1979 to 1998. The mapped region extends from 40°S to 40°N and from 70°E to 180°E.

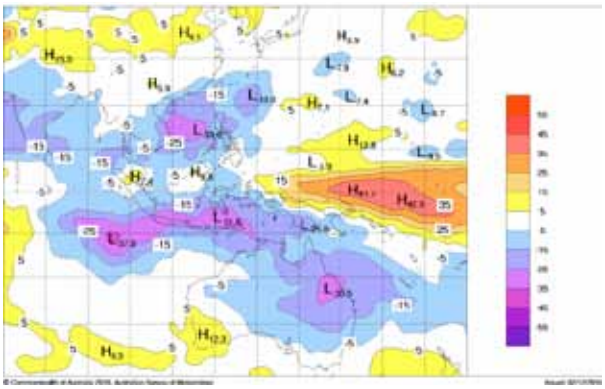

Fig. 4 Time-longitude section of daily-averaged OLR anomalies, averaged for 15°S–15°N, for the period from June 2010 to December 2010. Anomalies are with respect to a base period of 1979-2001.

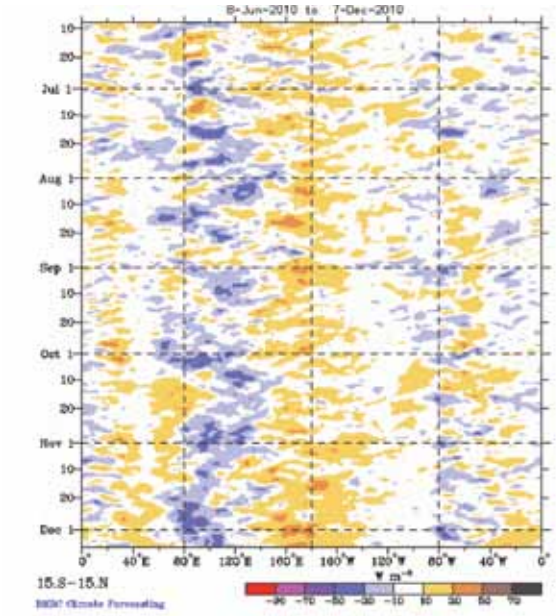

were also present across much of Australia, especially in the east; these areas experienced a much wetter than normal spring. In contrast, positive anomalies were present over southwestern Australia, which experienced a much drier than normal spring.

Madden-Julian Oscillation

The Madden-Julian Oscillation (MJO) is a tropical atmospheric anomaly which develops in the Indian Ocean and propagates eastwards into the Pacific Ocean (Donald et al. 2004). The MJO takes approximately 30 to 60 days to reach the western Pacific, with a frequency of six to twelve events per year (Donald et al. 2004). When the MJO is in an active phase, it is associated with increased tropical convection. The effects at this time of year are mainly concentrated in the northern hemisphere, however towards the end of spring the effect starts to become apparent in the southern hemisphere. The evolution of tropical convection anomalies along the equator with time is shown in Fig. 4, for the period from June 2010 to December 2010. In the daily averaged OLR anomalies in Fig. 4, September to November 2010 was generally a period of little activity for the MJO. However, some activity was evident during early October, when an eastward-propagating band of MJO-related convection was located in the Indian Ocean. The band strengthened and moved into Australian longitudes, then on into the western Pacific in mid-October before weakening and becoming indiscernible.

As discussed in the previous section, the positive OLR anomalies over the central equatorial Pacific may also be seen in Fig. 4. These positive anomalies are associated with the La Niña conditions, and became established during autumn 2010.

Oceanic patterns

Sea-surface temperatures

Spring 2010 global sea-surface temperature (SST) anomalies, from the US National and Oceanic and Atmospheric Administration Optimum Interpolation analysis (Reynolds et al. 2002), are displayed in Fig. 5, in degrees Celsius (°C). Positive (warm) anomalies are shown in red shades, while

Fig. 5 Global anomalies of sea-surface temperature (SST) for spring 2010 in °C. The contour interval is 0.5 °C, and the base period is 1961–1990.

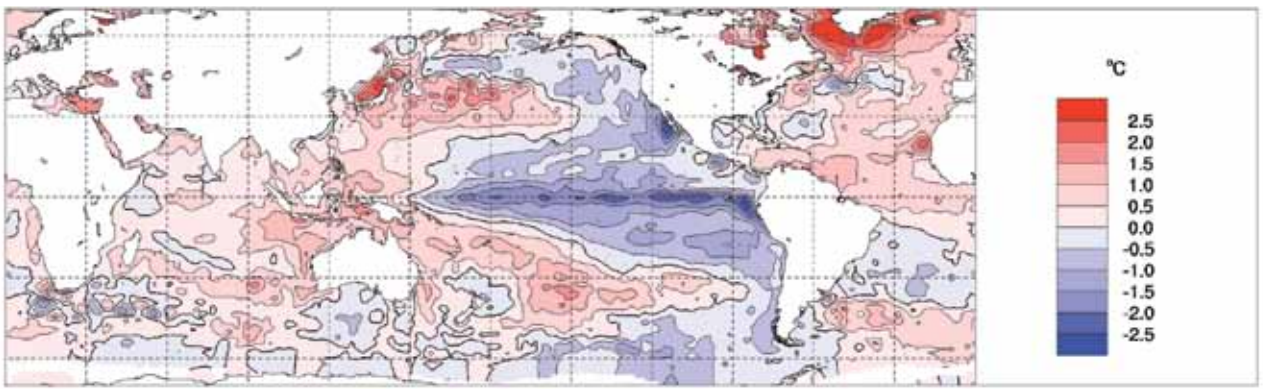

negative (cool) anomalies are shown in blue shades. During winter, the equatorial Pacific cooled rapidly, with the overall pattern being that of an emerging La Niña (Ganter, 2011). The cooling continued during spring as the La Niña strengthened. The strongest SST anomalies of –1.5 °C to –2.5 °C were located in a narrow band along the equator extending across much of the Pacific, while anomalies of more than –1.0 °C cover a large area of the eastern and central equatorial Pacific.

All three standard monthly NINO SST anomaly indices remained negative during spring. In the eastern Pacific, the NINO3 index cooled slightly from –0.99 ºC in August to –1.15 ºC in September, –1.53 °C in October and –1.44 ºC in November. Similarly, in the central Pacific, NINO 3.4 also continued to cool, from –1.21 ºC in August to –1.53 ºC in September, –1.60 °C in October and –1.43 °C in November. NINO4, located in the central to western Pacific, was a cool –0.92 ºC in August, cooling further to –1.27 °C in September, –1.35 °C in October and –1.31 °C in November.

In contrast SSTs were above average across the tropical Indian Ocean, except for a small region near the African coast. The Indian Ocean Dipole (IOD) is commonly measured by an index (Saji et al. 1999) that is the difference between the SST in the western (50°E to 70°E and 10°S to 10°N) and eastern (90°E to 110°E and 10°S to 0°S) equatorial Indian Ocean. A positive (negative) IOD period is characterised by cooler (warmer) than normal water in the tropical eastern Indian Ocean and warmer (cooler) than normal water in the tropical western Indian Ocean. At the start of spring the IOD was negative, remaining below the –0.4 ºC threshold until mid-October.

In the Australian region (a box from 0ºS to 50ºS and 94ºE to 174ºE), SSTs were extremely warm. Australian region SSTs for spring were the warmest on record (out of 111 years of record), with an anomaly of +0.61 °C, beating the previous record (1998) by 0.1 °C. The monthly values for September (+0.59 °C), October (+0.61 °C) and November (+0.62 °C) were all the highest on record[7].

Subsurface ocean patterns

The time-longitude section for the 20 ºC isotherm depth anomaly along the equator from January 2002 to November 2010, obtained from NOAA's TAO/TRITON data[8], is shown in Fig. 6. The 20 ºC isotherm depth is generally located close to the equatorial thermocline, which is the region of greatest temperature gradient with depth, and is the boundary between the warm near-surface and cold deep-ocean waters. Therefore, measurements of the 20 ºC isotherm depth make a good proxy for the thermocline depth. Positive (negative) anomalies correspond to the 20 ºC isotherm being deeper (shallower) than average. Changes in the thermocline depth may act as a precursor to subsequent changes at the ocean surface. A shallow thermocline depth results in more cold water available for upwelling, and therefore a potential cooling of surface temperatures.

Fig. 6 Time-longitude section of the five-day 20 ºC isotherm depth anomalies at the equator (2ºS–2ºN) from January 2002 (top of plot) to November 2010 (bottom). Units are metres. Plot produced by TAO Project Office/PMEL/NOAA.

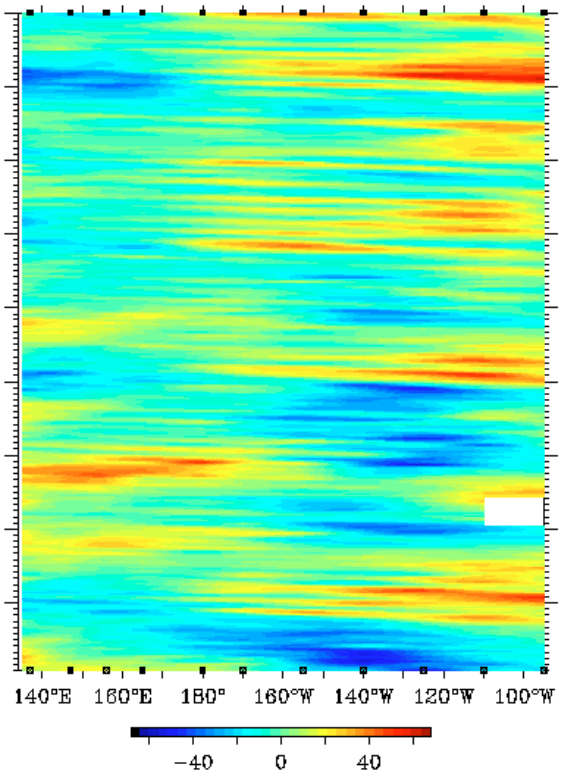

In winter 2010, the subsurface cooled across the central and eastern Pacific developing strongly negative 20 ºC isotherm anomalies, while the far western Pacific warmed, developing weak positive anomalies (Ganter 2011). This trend continued during spring, with the strong negative anomalies in the central and eastern Pacific remaining whilst the positive anomalies in the western Pacific strengthened slightly. The pattern of a shallower-than-normal 20 ºC isotherm in the central and eastern Pacific and a deeper-than-normal 20 ºC isotherm in the western Pacific is consistent with a La Niña event.

Figure 7 shows a cross-section of monthly equatorial subsurface anomalies from September to December 2010 (obtained from the National Meteorological and Oceanographic Centre). Red shading indicates positive anomalies, and blue shades indicate negative anomalies. The subsurface cross-section shows strong cool anomalies across the central and eastern Pacific in September after rapid cooling had occurred during the winter months. Strong cool anomalies remained throughout spring. The western Pacific had weak warm anomalies in August and continued to warm during the spring months.

[7]Data obtained from http://www.bom.gov.au/cgi-bin/climate/change/timeseries.cgi . Values are calculated from the NOAA Extended Reconstructed Sea Surface Temperature Version 3 (NOAA_ERSST_V3) data provided by the NOAA/OAR/ESRL PSD, from http://www.cdc.noaa.gov/ .
[8]Time-longitude section plot obtained from http://www.pmel.noaa.gov/tao/jsdisplay/

Fig. 7 Four-month (September to December 2010) sequence of vertical sea subsurface temperature anomalies at the equator for the Pacific Ocean. The contour interval is 0.5 °C.

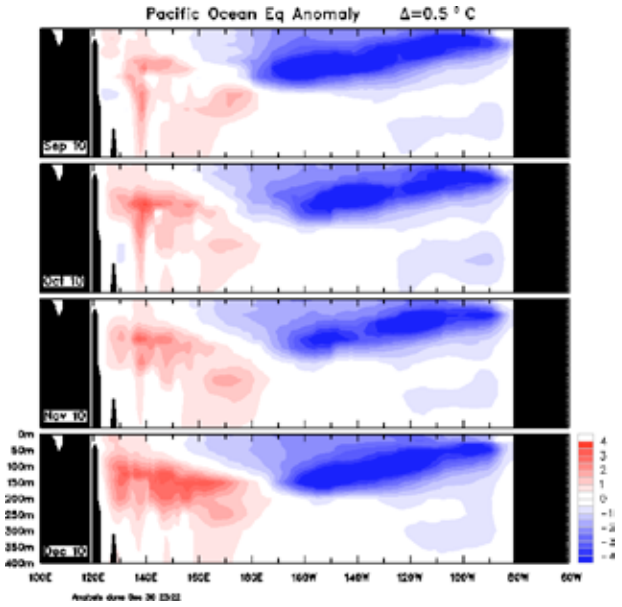

Global atmospheric patterns

Surface analyses

The southern hemisphere spring 2010 MSLP pattern, computed from the Bureau of Meteorology's Australian Community Climate and Earth-System Simulator[9] (ACCESS) model (the previous GASP model having been phased out in August 2010), is shown in Fig. 8, with the associated anomaly pattern shown in Fig. 9. These anomalies are the difference from a 1979–2000 climatology obtained from the National Centers for Environmental Prediction (NCEP) II Reanalysis data (Kanamitsu et al. 2002). The MSLP analysis has been computed using data from the 0000 UTC daily analyses of the ACCESS model. The MSLP anomaly field is not shown over areas of elevated topography (grey shading).

The spring MSLP pattern was zonal in the mid- to high latitudes, whilst maintaining the weak three-wave structure which developed during the winter months (Ganter, 2011). Troughs were located at approximately 130ºE, 90ºW and 30ºE. Anomalous high pressure occurred over the southern Atlantic Ocean, southern Indian Ocean and the western southern Pacific Ocean, with anomalies of more than +10.0 hPa in the southern Atlantic Ocean. MSLP was slightly above average over much of the Australian region, with anomalies of up to +5.0 hPa across most of the country and greater than +5.0 hPa over southern Western Australia with a maximum of +6.7 hPa just off the far southwest tip of Australia. Anomalous low pressure occurred over the Antarctic region, with anomalies of –12.5 hPa located around 100ºW.

[9]For more information on the Bureau of Meteorology's ACCESS model, see http://www.bom.gov.au/nwp/doc/access/NWPData.shtml

Fig. 8 Southern hemisphere spring 2010 MSLP (hPa). The contour interval is 5 hPa.

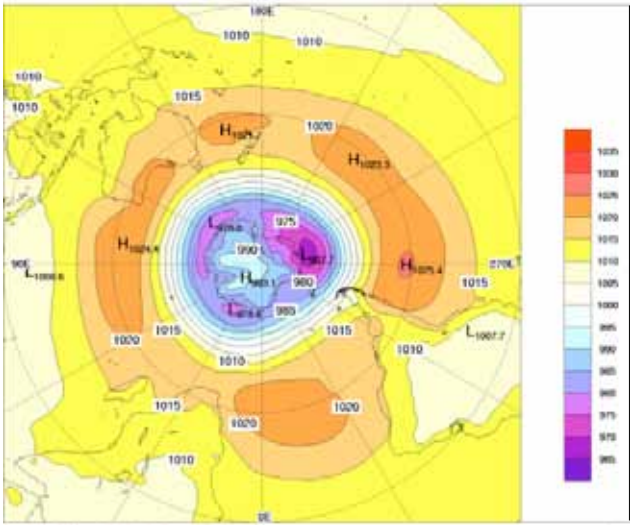

Fig. 9 Southern hemisphere spring 2010 MSLP anomalies (hPa). The contour interval is 2.5 hPa.

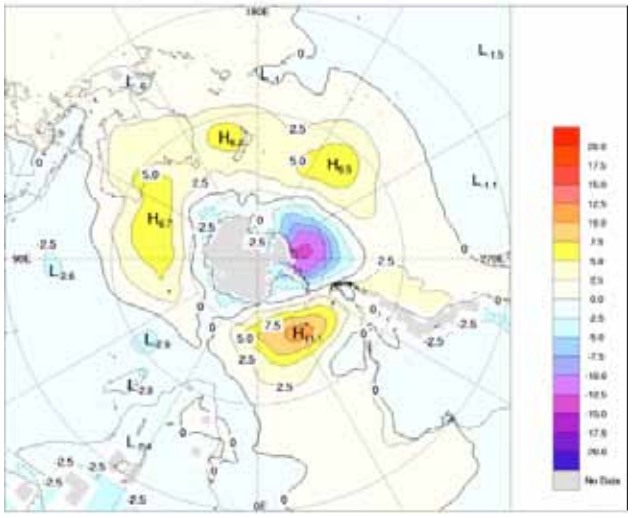

This pattern has strong similarities to the loading pattern of the Southern Annular Mode (SAM) which is discussed in more detail in a following section.

Mid-tropospheric analyses

The 500 hPa geopotential height, which is an indicator of the steering of surface synoptic systems across the southern hemisphere, is shown in Fig. 10 for spring 2010. The associated anomalies are shown in Fig. 11. Figure 10 shows that the spring 500 hPa height pattern displays the characteristic zonal structure in the mid- to high latitudes, with weak three-wave characteristics that were also noted in Fig. 8. The anomaly field shown in Fig. 11 shows that the strong negative anomaly around 100ºW and positive anomalies in the southern Atlantic Ocean, southern Indian Ocean and the southwestern Pacific Ocean apparent at the surface (Fig. 9.) are also visible at this level.

Fig. 10 Southern hemisphere spring 2010 500 hPa mean geopotential height (gpm). The contour interval is 100 gpm.

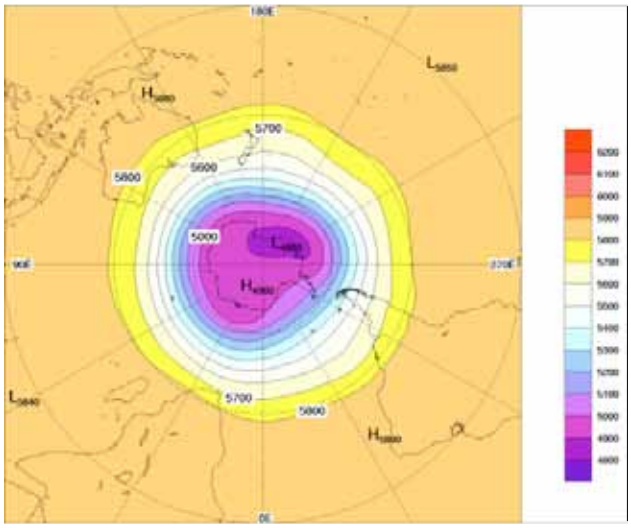

Fig. 11 Southern hemisphere spring 2010 500 hPa mean geopotential height anomaly (gpm). The contour interval is 30 gpm.

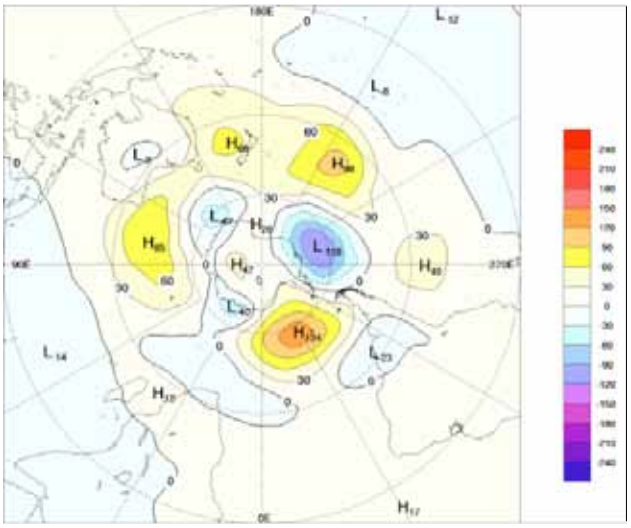

Southern Annular Mode

The Southern Annular Mode (SAM) describes the periodic, approximately ten-day, oscillation of atmospheric pressure between the polar and mid-latitude regions of the southern hemisphere. Positive phases of SAM are characterised by increased atmospheric mass over the extra-tropics, decreased atmospheric mass over Antarctica and a poleward contraction of the mid-latitude band of westerly winds. Conversely, negative phases of SAM relate to reduced mass over the extra-tropics, increased mass over Antarctica and an equatorward expansion of the mid-latitude band of westerly winds. A similar oscillation exists in the northern hemisphere, the Northern Annular Mode, or NAM. After becoming strongly positive in winter, the Climate Prediction Center standardised monthly SAM index (Climate Prediction Center, 2010), which is calculated using NCEP-NCAR reanalysis data, remained positive during the spring. The November value of +1.52 was the strongest November value on record (records began in 1979).

Monthly values of an observations-based SAM index[10] (Marshall 2003) indicate a slight dip into negative values in September (–0.33) before a return to strongly positive values in October and November (+3.19 and +3.88 respectively). The seasonal value of +2.25 for spring 2010 is the highest spring value on record (records began in 1957).

Figures 9 and 11 indicate anomalously high pressure for spring 2010 around the mid-latitudes in the southern Indian Ocean, Atlantic Ocean and Pacific Ocean regions and anomalously low pressure over the Antarctic region. As discussed in an earlier section, this pattern is very similar to the loading pattern for positive SAM. Hendon et al. (2007) discuss Australian rainfall patterns associated with the positive and negative phases of SAM. Their findings report that the positive phase of SAM is usually associated with decreased westerly flow in the southern regions of Australia. In the spring months, this can result in reduced rainfall over western Tasmania, and increased rainfall along the coast of New South Wales. During spring 2010, the effect of the La Niña was dominant in determining rainfall patterns in these regions. Whilst the positive SAM contributed to the spring rainfall in southeastern Australia, some evidence of the climatic effects of the SAM was hidden by the strong La Niña.

Blocking

The time-longitude section of the daily southern hemisphere blocking index (BI, Wright 1993) is shown in Fig. 12, with the start of the season beginning at the top of the plot. This index is a measure of the strength of the zonal 500 hPa flow in the mid-latitudes (40ºS to 50ºS) relative to that at lower (25ºS to 30ºS) and higher (55ºS to 60ºS) latitudes. Positive values of the blocking index are generally associated with a split in the mid-latitude westerly flow centred near 45ºS and mid-latitude blocking activity. Blocking activity most commonly occurs in the Australian and western Pacific latitudes. Figure 13 shows the seasonal index for each longitude.

The seasonal index shows that blocking was generally close to average in most areas, apart from the Indian Ocean and Atlantic Ocean regions which were slightly above average. Positive daily BI values were consistent throughout the spring season between 150ºE to 150ºW (Tasman Sea and Western Pacific Ocean) and 20ºW to 70ºW (Atlantic Ocean), with similar strength peak values in both these areas.

Winds

Spring 2010 low-level (850 hPa) and upper-level (200 hPa) wind anomalies (as per the surface analyses, computed from

[10]Values obtained from the British Antarctic Survey http://www.nerc-bas.ac.uk/icd/gjma/sam.html

Fig. 12 Spring 2010 daily blocking index time-longitude section. Day 1 is 1 September.

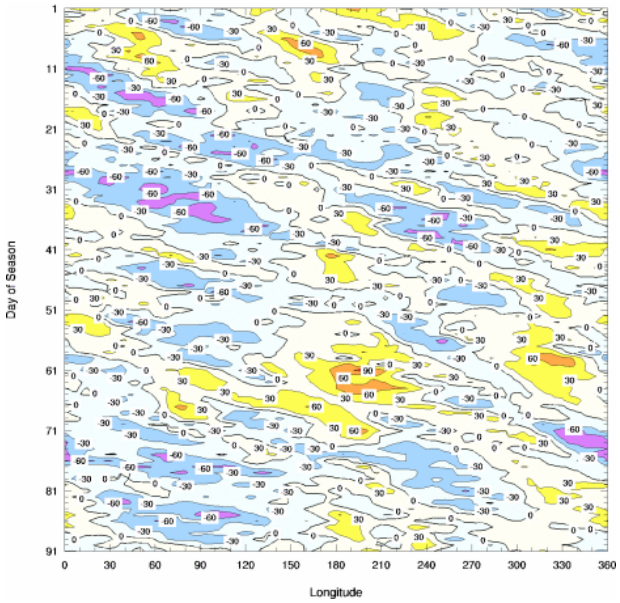

Fig. 13 Mean southern hemisphere blocking index for spring 2010 (solid line). The dashed line shows the corresponding long-term average. The horizontal axis shows the degrees east of the Greenwich meridian.

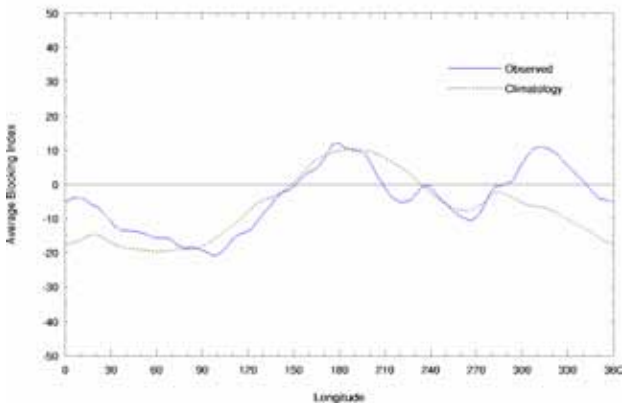

ACCESS and anomalies with respect to the 22-year NCEP II climatology) are shown in Figs. 14 and 15, respectively. Isotach contours are at 5 ms^{-1} intervals.

The low-level winds reflected the MSLP anomalies shown in Fig. 9, with an anticyclonic anomaly over the southern Indian Ocean, to the southwest of Western Australia, and another in the Tasman Sea. The enhanced easterlies over the western to central Pacific (anomalies of between 5 and 10 ms^{-1} are apparent near Papua New Guinea), in combination with enhanced upper-level westerlies across the same region, were indicative of a stronger than normal Walker Circulation (La Niña conditions) and are consistent with the La Niña conditions evident in the SSTs.

Australian region

Rainfall

Australian rainfall totals for spring are shown in Fig. 16, while the rainfall deciles for the same period are shown in Fig. 17. The rainfall deciles are calculated using all springs from 1900 to 2010.

Spring 2010 was Australia's wettest spring on record (out of 111 years of record). Overall, Australia had a wetter than normal spring, with an area-average of 166.9 mm, 130 per cent above the long-term average (1961–1990). Figure

Table 1. Summary or the seasonal rainfall ranks and extremes on a national and State basis for spring 2010. The ranking in the last column begins from 1 (lowest) to 111 (highest) and is calculated over the years 1900 to 2010 inclusive.

Region	*Highest seasonal total (mm)*	*Lowest seasonal total (mm)*	*Highest daily total (mm)*	*Area-averaged rainfall (mm)*	*Rank of area-averaged rainfall*
Australia	3209.6 at Bellenden Ker Top Stn (Qld)	Zero at several locations	363.0 at Wilson Beach (Qld) on 20/09	166.9	111
Western Australia	387.3 at Theda	Zero at several locations	121.2 at Faraway Bay on 14/10	67.5	104
Northern Territory	582.9 at Lake Evella	34.8 at Centre Island	170.0 at Mataranka on 31/10	177.2	111
South Australia	317.0 at Parawa	41.1 at Woomera (Arcoona)	138.0 at Bowmans (Pigeldee) on 15/10	133.1	111
Queensland	3209.6 at Bellenden Ker Top Stn	Zero at Bowthorn Station	363.0 at Wilson Beach on 20/09	256.1	111
New South Wales	1049.0 at Belleview Park	76.6 at Delegate River	225.0 at Meerschaumvale on 04/10	258.4	111
Victoria	895.8 at Falls Creek (Rocky Valley)	114.7 at Walpa (Danyo)	135.2 at Whitlands on 05/09	267.7	105
Tasmania	1164.2 at Mt Read	119.2 at Mathinna (South Esk River)	84.4 at Erriba on 31/10	419.9	81

Fig. 14 Global spring 2010 850 hPa vector wind anomalies (m s^{-1}).

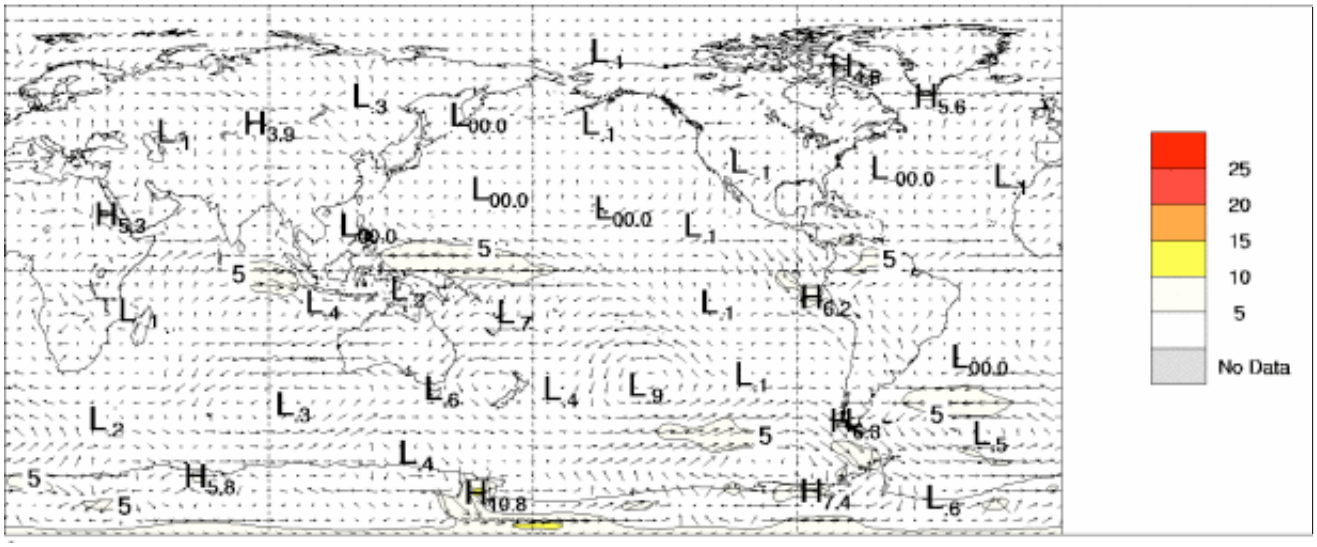

Fig. 15 Global spring 2010 200 hPa vector wind anomalies (m s^{-1}).

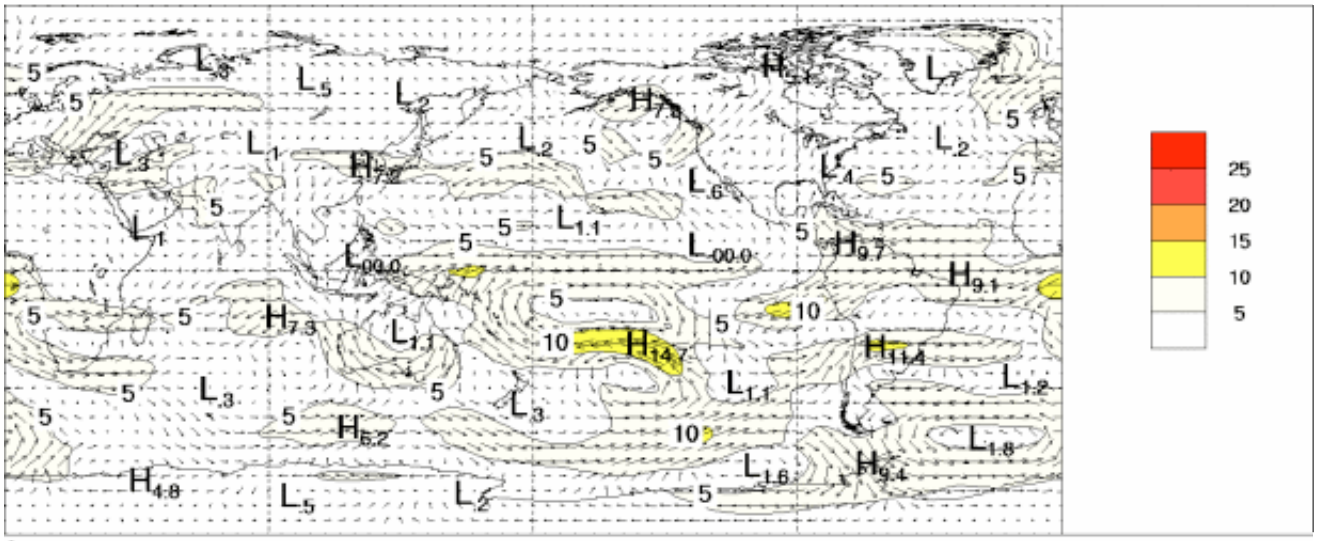

Fig. 16 Spring 2010 rainfall totals (mm) for Australia.

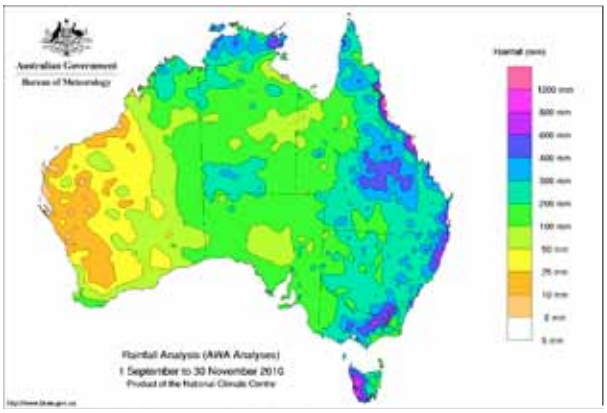

Fig. 17 Spring 2010 rainfall deciles for Australia: decile ranges based on grid-point values over spring periods from 1900 to 2010.

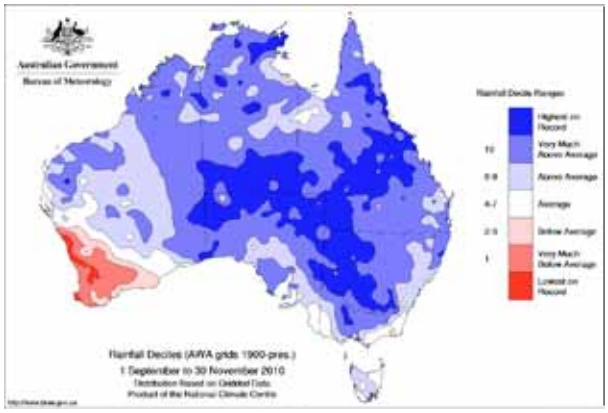

17 shows that most regions received above to very much above average falls, whilst a large area (about twenty-two per cent of the country) received the highest totals on record. Only southwest Western Australia and a small part of East Gippsland in Victoria reported below average rainfall.

Queensland, New South Wales, South Australia and the Northern Territory all recorded their wettest spring on record. Major flooding was reported in many of these regions during the season, most notably in northern Victoria in early September, and southeast Queensland and the Riverina and South West Slopes regions of New South Wales in mid-October.

In sharp contrast, southwest Western Australia received rainfall which was very much below average, with some areas reporting the lowest spring rainfall on record. For this region (the area southwest of a line joining the points 30°S, 115°E and 35°S, 120°E), spring 2010 was the driest on record with an area average of 67.5 mm (previous record was 71.2 mm, set in 1969), and followed the driest winter on record (Ganter 2011).

September was Australia's wettest September on record, whilst October was the second wettest on record. November was also in the top ten wettest on record (7th wettest).

Drought

As discussed in the previous section, rainfall was below to very much below average across southwestern Australia. Persistent dry weather in southwest Western Australia produced the driest spring on record for the southwest Western Australia region as a whole, and followed the driest winter on record. Further east, rainfall has generally been above average since late 2009 for northern and eastern Australia, alleviating any previous short-term rainfall deficiencies.

A way in which the Bureau of Meteorology presently assesses drought is by considering the extent of areas of the country which contain accumulated rainfall in the lowest decile for varying timescales.

For the three months of spring ending November 2010, 3.1 per cent of Australia had experienced rainfall at or below the 10th percentile (serious deficiency), with 2.1 per cent of the country experiencing severe deficiency (rainfall at or below the 5th percentile). Lowest rainfall on record was received by 0.56 per cent of the country during this period. These areas were located entirely within southwestern Australia.

The national figure of 3.1 per cent (serious deficiency) for the three months ending November 2010 has shown a slight reduction from the 3.7 per cent for the three months ending August 2010, and is significantly smaller than the 13.1 per cent for the three months ending November 2009.

For the twelve-month period ending November 2010, 5.1 per cent of Australia was experiencing serious deficiency whilst 3.1 per cent of the country was under severe deficiency. Lowest rainfall on record was seen by 0.99 per cent of the country over this period. These areas were confined to western parts of Western Australia, with the largest and most severe deficiencies located in southwestern Western Australia. The area experiencing lowest on record rainfall was located entirely within southwestern parts.

Temperature

Figure 18 shows maximum and minimum temperature anomalies for spring. Seasonal anomalies are calculated with respect to the 1961–1990 period, and use all stations in the data archive for which an elevation is available. Station normals have been estimated using gridded climatologies for those stations with insufficient data within the 1961–1990 period to calculate a station normal directly. Figure 19 shows maximum and minimum temperature deciles, calculated using monthly temperature analyses from 1911 to 2010.

Spring mean maximum temperatures were generally below average across most of the country, with the exception of western Western Australia which was warmer than average. Nationally-averaged maximum temperatures were 1.23 °C below normal for spring, making it Australia's fourth-coldest spring on record. Maximum temperature anomalies of between –2 and –5 °C were widespread across central Australia. A large part of this region observed record low maxima, an area totalling about fifteen per cent of the country as a whole. Areas of lowest on record include a large region

Fig. 18 Spring 2010 temperature anomalies (°C) for Australia: anomalies based on a 1961–1990 mean. (a) maximum temperature anomalies. (b) minimum temperature anomalies.

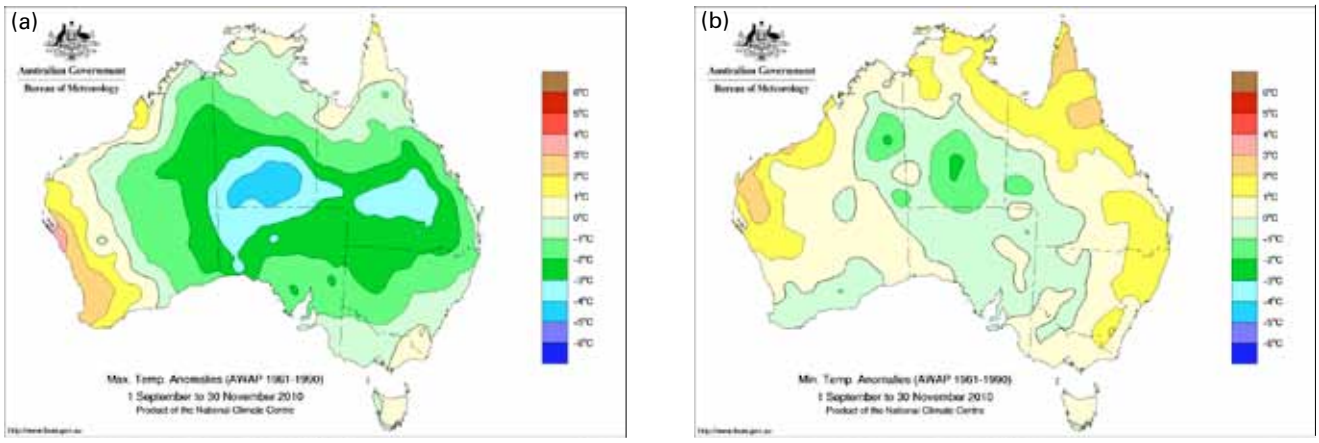

Fig. 19 Spring 2010 temperature deciles for Australia: decile ranges based on grid-point values over the spring periods for 1911 to 2010. (a) maximum temperature deciles. (b) minimum temperature deciles.

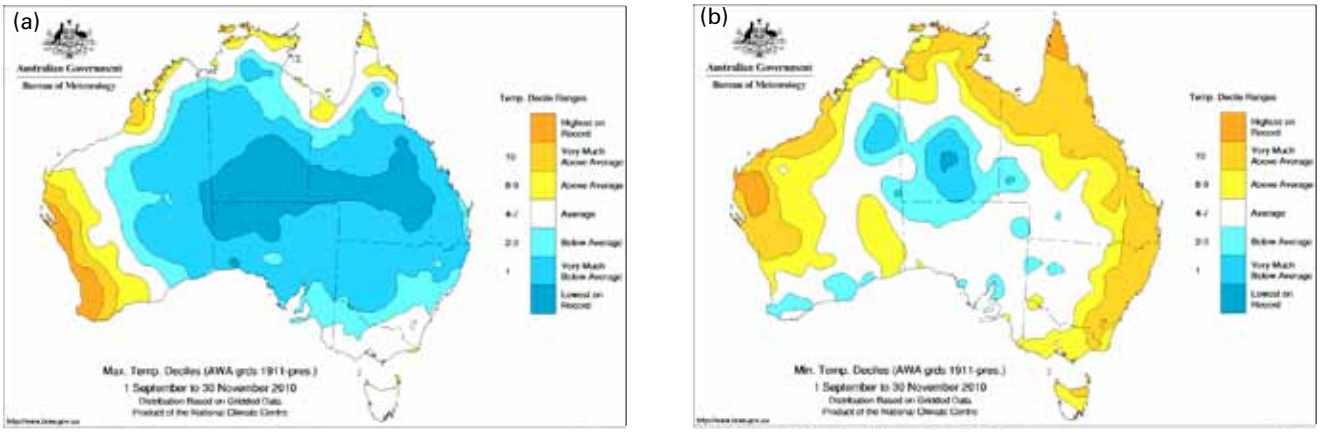

Table 2. Summary of the seasonal maximum temperature ranks and extremes on a national and State basis for spring 2010. The ranking in the last column begins from 1 (lowest) to 61 (highest) and is calculated over the years 1950 to 2010. Fractional ranks denote tied values.

Region	*Highest seasonal mean maximum (°C)*	*Lowest seasonal mean maximum (°C)*	*Highest daily temperature (°C)*	*Lowest daily maximum temperature (°C)*	*Area-averaged temperature anomaly (°C)*	*Rank of area-averaged temperature anomaly*
Australia	38.0 at Fitzroy Crossing (WA)	6.9 at Mt Hotham (Vic)	46.9 at Roebourne (WA) on 10/11	–2.6 at Mt Hotham (Vic) on 16/09	–1.23	4
Western Australia	38.0 at Fitzroy Crossing	19.5 at Albany	46.9 at Roebourne on 10/11	10.9 at Kalgoorlie-Boulder on 01/09	–0.29	21
Northern Territory	37.9 at Bradshaw	25.5 at Kulgera	42.8 at Rabbit Flat on 09/11	11.1 at Arltunga on 16/09	–1.91	1
South Australia	27.5 at Marree Comparison	15.0 at Mt Lofty	40.9 at Nullabor on 11/11	7.1 at Mt Lofty on 15/10	–2.16	3
Queensland	36.1 at Century Mine	19.7 at Applethorpe	42.0 at Urandangi on 05/10	10.9 at Applethorpe on 16/10	–1.77	2
New South Wales	26.4 at Lightning Ridge	7.5 at Thredbo	39.2 at Menindee on 12/11	–1.8 at Thredbo on 16/10	–1.14	7
Victoria	22.6 at Mildura	6.9 at Mt Hotham	37.5 at Mildura on 12/11	–2.6 at Mt Hotham on 16/09	–0.34	22.5
Tasmania	18.1 at Launceston	7.2 at Mt Read	34.8 at Campania (Kincora) on 23/11	–2.2 at Mt Wellington on 28/09	+0.42	40

encompassing central Queensland, reaching across most of the southern Northern Territory, and over the South Australia border, as well as a small area just south of Cook in South Australia. The cooler maximum temperatures resulted in the Northern Territory recording its coldest spring maximum temperature on record (–1.91 °C), Queensland its second-coldest (–1.77 °C), and South Australia its third-coldest (–2.16 °C). Widespread heavy rainfall in central Australia (Fig. 17) contributed to the cooler daytime temperatures.

Above average maxima were mostly confined to the western part of Western Australia. The Cape York Peninsula in Queensland and small areas along the northern coast of the Top End in the Northern Territory were also slightly warmer than average. Temperatures of at least 1 °C above normal were observed in a region south of Port Hedland in Western Australia, and reaching in as far inland as Southern Cross. Part of this area, stretching along the coastline, had record high maximum spring temperatures. Two small regions near Broome in Western Australia and the tip of the Cape York Peninsula also recorded daytime temperatures of at least 1 °C above normal.

Nationally averaged minimum temperatures were near normal, with an anomaly of +0.15 °C. Negative anomalies were generally in central and southern Australia, with positive anomalies in the tropical north, and broad regions across the western and eastern coasts. Notable cooler than normal

Table 3. Summary of the seasonal minimum temperature ranks and extremes on a national and State basis for spring 2010. The ranking in the last column begins from 1 (lowest) to 61 (highest) and is calculated over the years 1950 to 2010. Fractional ranks denote tied values.

Region	*Highest seasonal mean minimum (ºC)*	*Lowest seasonal mean minimum (ºC)*	*Highest daily minimum temperature (ºC)*	*Lowest daily temperature (ºC)*	*Area-averaged temperature anomaly (ºC)*	*Rank of area-averaged temperature anomaly*
Australia	27.2 at Troughton Island (WA)	0.2 at Mt Wellington (Tas)	31.9 at Telfer (WA) on 24/11	–12.1 at Charlotte Pass (NSW) on 08/09	+0.15	32
Western Australia	27.2 at Troughton Island	5.5 at Newdegate	31.9 at Telfer on 24/11	–3.6 at Eyre on 08/10	+0.26	34.5
Northern Territory	26.1 at Cape Don	11.9 at Arltunga	29.9 at Yuendumu on 04/10	3.3 at Alice Springs on 20/09	–0.94	7
South Australia	14.7 at Oodnadatta	6.2 at Yongala	27.3 at Marree Comparison and Oodnadatta on 12/11	–1.8 at Keith (Munkora) on 25/10	–0.18	21.5
Queensland	26.0 at Horn Island	10.1 at Applethorpe	29.4 at Mornington Island on 18/11	0.9 at Applethorpe on 07/09	+0.79	54
New South Wales	17.1 at Byron Bay	0.4 at Thredbo	24.5 at Broken Hill on 12/11	–12.1 at Charlotte Pass on 08/09	+0.48	41
Victoria	11.7 at Gabo Island	0.9 at Mt Hotham	24.0 at Mildura on 12/11	–7.6 at Mt Hotham on 08/09 and on 16/10	+0.52	54
Tasmania	10.5 at Swan Island	0.2 at Mt Wellington	18.2 at St Helens on 25/11	–7.9 at Liawenee on 07/09	+0.22	45

minimum temperatures were mostly confined to the interior of the continent, with anomalies of between –1 and –3 °C in a wide area surrounding Alice Springs. A small region within this area observed lowest-on-record minimum temperatures. Smaller areas near Birdsville in Queensland and Halls Creek and Giles in Western Australia also recorded anomalies of –1 °C.

Minimum temperatures of 1 ºC above normal were reported along the central west coast of Western Australia, across the tropical north, and over a large region from Bundaberg in Queensland down to the Victoria/New South Wales border, reaching as far inland as Charleville in Queensland. The central west coast of Western Australia and the Cape York Peninsula recorded anomalies of at least +2 ºC. These two regions, as well as the Cobourg Peninsula in the Northern Territory, also had areas of highest-on-record minima.

References

Campbell, B. 2011. Seasonal climate summary southern hemisphere (autumn 2010): rapid decay of El Niño, wetter than average in central, northern and eastern Australia and warmer than usual in the west and south. *Aust. Met. Oceanogr. J., 61,* 65–76.

Climate Diagnostics Center. 2010. *Historical ranks of the MEI,* http://www.cdc.noaa.gov/people/klaus.wolter/MEI/rank.html.

Climate Prediction Center. 2010. *Monthly mean AAO index since January 1979,* http://www.cpc.noaa.gov/products/precip/CWlink/daily_ao_index/aao/aao.shtml.

Donald, A., Meinke, H., Power, B., Wheeler, M. and Ribbe, J. 2004. Forecasting with the Madden-Julian Oscillation and the applications for risk management. In: *4th International Crop Science Congress,* 26 September – 01 October 2004, Brisbane, Australia.

Ganter, C. 2011. Seasonal climate summary southern hemisphere (winter 2010): A fast developing La Niña. *Aust. Met. Oceanogr. J., 61,* 125–135.

Hendon, H.H., Thompson, D.W.J. and Wheeler, M.C. 2007. Australian Rainfall and Surface Temperature Variations Associated with the Southern Hemisphere Annular Mode. *J. Clim., 20,* 2452–67.

Kanamitsu, M., Ebisuzaki, W., Woollen, J., Yang, S.-K., Hnilo, J.J., Fiorino, M. and Potter, G.L. 2002. NCEP-DOE AMIP-II Reanalysis (R-2). *Bull. Am. Meteorol. Soc., 83,* 1631–43.

Kuleshov, Y., Qi, L., Fawcett, R. and Jones, D. 2008. On tropical cyclone activity in the Southern Hemisphere: trends and the ENSO connection. *Geophys. Res. Lett., 35,* L14S08, doi:10.1029/2007GL032983

Marshall, G.J. 2003. Trends in the Southern Annular Mode from Observations and Reanalyses. *J. Clim., 16,* 4134–4143.

Reynolds, R.W., Rayner, N.A., Smith, T.M., Stokes, D.C. and Wang, W. 2002. An improved in situ and satellite SST analysis for climate. *J. Clim., 15,* 1609–25.

Saji, N.H., Goswami, B.N., Vinayachandran, P.N., Yamagata, T., 1999. A Dipole Mode in the Tropical Indian Ocean, *Nature, 401,* 360–363.

Troup, A.J. 1965. The Southern Oscillation. *Q. J. R. Meteorol. Soc., 91,* 490–506.

Wolter, K. and Timlin, M.S. 1993. Monitoring ENSO in COADS with a seasonally adjusted principal component index. *Proc. of the 17th Climate Diagnostics Workshop*, Norman OK, NOAA/NMC/CAC, NSSL, Oklahoma Clim. Survey, CIMMS and the School of Meteorology, Univ. of Oklahoma, 52–7.

Wolter, K. and Timlin, M.S. 1998. Measuring the strength of ENSO – how does 1997/98 rank? *Weather, 53,* 315–24.

Wright, W.J. 1993. Seasonal climate summary southern hemisphere (autumn 1992): signs of a weakening ENSO event. *Aust. Meteorol. Mag., 42,* 191–8.